This article has been accepted for publication in a future issue of this journal, but has not been fully edited.
Content may change prior to final publication in an issue of the journal. To cite the paper please use the doi provided on the Digital Library page.

Multi-Binding Biotinylated Iron Oxide Nanoparticles (biotin-IONPs) as a Promising Versatile Material for Magnetic Biomedical Applications

Y. Du[1] *and P. W. T. Pong*[1*]

[1] *The University of Hong Kong, Pokfulam Road, Hong Kong, China*
E-mail: ppong@eee.hku.hk

The tetrameric streptavidin and avidin both have four sites that can specifically bind with biotin. Taking advantage of this high affinity binding, it is possible to realize multi-binding of biotinylated nanoparticles to avidin or streptavidin molecules. The iron oxide nanoparticles (IONPs) have been actively investigated in biomedical applications. In this study, biotin-IONPs with around 10.5 nm magnetic core size were synthesized. They exhibited long-term hydrophilic stability, and the activity of the biotin content were verified by avidin-HRP induced chromogenic experiment. These biotin-IONPs were then studied as magnetic labels in substrate-based and substrate-free magnetic bio-labeling scheme of alpha-fetoprotein (AFP). The multi-binding ability of these biotin-IONPs with streptavidin functionalized detection antibody (streptavidin-detection antibody) were proved both on microplate well surfaces and in solution. Consequently, biotin-IONPs are promising magnetic label materials for the improvement of magnetic biodetection. In addition, the avidin-induced biotin-IONP assemblies were produced in MilliQ water solution and in water-in-oil microemulsion system. In summary, based on their multi-binding nature, the biotin-IONPs can be considered as a versatile material to improve the sensitivity of magnetic biodetection, and to be further built into assemblies for future biomedical applications such as magnetic resonance imaging (MRI) and target drug delivery.

Key words: Iron oxide nanoparticles (IONPs), biotin, magnetic biodetection

1. Introduction: Magnetic iron oxide nanoparticles (IONPs) have gathered great interests in the area of biomedical applications due to their bio-compatibility, ease of synthesis, environmental friendly, and low cost [1-3]. They have played various roles in biomedical applications, such as magnetic labels in magnetic biodetection technology [1], contrast agents in magnetic resonance imaging (MRI) [4], and magnetic carriers in target drug delivery [5]. In order to prevent the steric hindrance, IONPs with small size which is comparable with biological molecules have been generally desired in biological practices [6]. However, the small size greatly limited the intensity of the magnetic signal caused by IONPs. This contradiction between magnetic signal and biological performance may hinder the further development of the corresponding diagnostic and therapeutic technologies. It is worthwhile to develop an approach to amplify the IONP magnetic signals without enlarging IONP size, and finally, to improve the performance of magnetic IONPs in their biomedical applications.

The magnetic biodetection devices are a combination of micro-/nano-electronic techniques and magnetic labels, and magnetic IONPs have been widely utilized as magnetic label materials. Generally, magnetic biodetection devices detect the specific binding of magnetic labels with target biomolecules based on two categories of magnetic biosensing principles: the substrate-based principles and substrate-free principles [7]. The substrate-based devices, such as giant magnetoresistance (GMR) biosensors, detect the binding of magnetic labels with biomolecules immobilized on sensor surfaces [8]. The substrate-free devices, such as Brownian relaxation biosensors, detect the binding of magnetic labels with the biomolecules suspended in solution [9]. Magnetic labels with size comparable with DNA or protein molecules, usually under 20 nm, have been reported to be more desirable for magnetic biodetection [10]. However, it is a challenge to detect such tiny magnetic labels due to their limited magnetic moments [6]. The sensitivity of both of these two groups of devices can be improved by realizing multi-binding of the magnetic labels with each target biomolecule. In previous studies, an amplification step was always included by tethering several secondary magnetic labels to the originally captured magnetic label [11]. However, since it is difficult to control the number of captured secondary magnetic labels, this amplification method may harm the quantitative relationship between the number of magnetic labels and the actual biorecognition events. To this end, it is meaningful to develop the multi-binding of original magnetic labels to target biomolecules with controllable quantitative relationship.

Streptavidin and biotin are a ligand-receptor pair with high affinity [12]. In the context of magnetic biodetection, this streptavidin-biotin system can act as a bridge between magnetic labels and biomolecules to create a robust magnetic biolabeling scheme [13]. In recent years, development of magnetic biosensors was mostly based on streptavidin-functionalized magnetic nanoparticles [11]. However, by utilizing streptavidin-functionalized magnetic nanoparticles, each biotinylated biomolecule is specifically bound with only one nanoparticle [14, 15]. On the contrary, more than one biotinylated magnetic nanoparticles can bind to each streptavidin-functionalized biomolecule since each streptavidin molecule has four binding sites for biotin [16]. Consequently, by adopting biotinylated magnetic nanoparticles, multi-binding of original magnetic labels can be realized. In addition, the avidin, which are also the receptor of biotin, also has four binding sites for biotin, and thus, can induce crosslinking of biotinylated nanoparticles [17]. By extending this multi-binding strategy into IONP studies, it is possible to build IONP assemblies with suitable morphologies for specific biomedical applications, such as MRI and target drug delivery.

In this study, biotinylated IONPs (biotin-IONPs) were synthesized as a potential versatile material for magnetic biomedical applications. The feasibility of realizing multi-binding of biotin-IONPs were studied. Biotin-IONP serving as magnetic labels were studied in magnetic bio-labeling scheme performed on substrate surfaces and in aqueous solution. The avidin-induced biotin-IONP assemblies based on the multi-binding nature were also investigated.

2. Experiments:

2.1. Materials: FeO(OH), oleic acid, 1-octadecene, chloroform, and bovine serum albumin (BSA) were purchased from Sigma-Aldrich. DSPE-PEG(2000)Biotin (10 mg/mL) was obtained from Avanti Polar Lipids. The 96-well microplates were purchased from Corning. The alpha-fetoprotein (AFP) (Human Alpha Fetoprotein (AFP) Antigen

Grade [A01406H]) and a pair of antibodies to AFP, capture antibody (Monoclonal Antibody to Human Alpha Fetoprotein [MAM01-301]) and detection antibody (Goat Antibody to Human Alpha Fetoprotein (AFP) [K92270G]), were all purchased from Meridian. Lightning-Link® Streptavidin Conjugation Kit was purchased from Innova Biosciences. The avidin-HRP (horseradish peroxidase), biotin-HRP, TMB (3,3',5,5'-Tetramethylbenzidine), and stop solution were obtained from Neobioscience. The avidin was purchased from ThermoFisher Scientific. The dynamic light scattering (DLS) measurements were performed using a Malvern Zeta Sizer Nano ZS-90 instrument. Transmission electron microscopy (TEM) was performed on a Philips CM100 Transmission Electron Microscope. The optical density (OD) signals were measured by a Molecular Devices VERSA max microplate reader.

2.2. Synthesis and characterization of biotin-IONPs: IONPs were synthesized by a one-pot thermal decomposition method in a three-neck flask equipped with magnetic stirrer, condenser, thermocouple and heating mantle [18]. FeO(OH) fine powder and oleic acid with molar ratio of 1:4 was dissolved in 1-octadecene, the mixture was added into the flask and magnetically stirred under a flow of nitrogen. This mixture was then heated under stirring to 285℃ and refluxed at this temperature for 1.5 h. This thermal decomposition reaction was protected under nitrogen in order to avoid undesired side-reactions (e.g. oxidation of oleic acid).

The IONP surfaces were then functionalized by biotin utilizing a surfactant addition approach [19]. The synthesized nanoparticles were dissolved in chloroform to form solution with concentration of 1 mg particles/mL. Subsequently, 1 mL of this IONP solution was mixed with 0.5 mL of the chloroform solution of DSPE-PEG(2000)Biotin, and this mixture was shaken for 1 h. The solvent chloroform was then evaporated giving black solid residue of biotin-IONPs. The black product was then dispersed in phosphate buffered saline (PBS) solution or MilliQ water for further experiments. This surfactant addition approach can produce a cell-membrane-like double-layer structure over the nanoparticle surface [19]. The morphology and size distribution of the as-synthesized IONPs and biotin-IONPs were then analyzed using TEM.

The activity of biotin on nanoparticle surfaces was verified by a colorimetrical method. The biotin-IONP solutions in PBS with a series of concentrations (0, 1, 5, 10, 50, and 100 ng IONP/mL) were added into the wells of a 96-well microplate. The plate was then glued on the surface of a strong magnet. Thereafter, the microplate was stored at 4℃ overnight, and the biotin-IONPs were magnetically attracted to the bottom of the wells. Then, 33 ng/mL avidin-HRP (horseradish peroxidase) solutions were added into the wells and incubated at 36 ℃ for 10 min to specifically tag the biotin-IONPs through the avidin-biotin binding. After washing away the free avidin-HRP, the chromogenic substrate of HRP, TMB (3,3′,5,5′-Tetramethylbenzidine), was introduced. HRP induced the colorless TMB solution turned into blue. At the end of reaction, stop solution was added to stop the reaction and turn the blue solutions into yellow. The colored solutions were measured using a microplate reader at wavelength of 450 nm. A control experiment was also performed with the same procedure except that avidin-HRP was replaced by biotin-HRP.

2.3. Investigation of the multi-binding ability of biotin-IONPs with streptavidin-detection antibody as magnetic label material: In this study, the as-synthesized biotin-IONPs were tested as magnetic labels in the magnetic bio-labeling scheme for AFP in both substrate-based and substrate-free manner. In order to bind with biotin-IONPs, the detection antibodies have been previously functionalized with streptavidin using Lightning-Link® Streptavidin Conjugation Kit to produce streptavidin-detection antibody. In the substrate-based study, solutions of capture antibody, AFP, and streptavidin-detection antibody were sequentially added into a 96-well microplate for incubation to build the sandwich-configured immunoassay, capture antibody/AFP/streptavidin-detection antibody [20]. Subsequently, the biotin-IONP solution was added and biotin-IONPs were captured by the immobilized streptavidin-detection antibodies. In order to investigate the multi-binding ability, biotin-IONP solutions with high (1 μg IONPs/mL), median (0.1 μg IONPs/mL), and low (0.01μg IONPs/mL) concentration were tested. The quantity of captured biotin-IONPs was also studied using the HRP-induced colorimetrical method. The avidin-HRP was introduced to tag the biotin-IONPs, and after washing away the free avidin-HRP, the chromogenic substrate TMB was introduced. At the end of the reaction, stop solution was added and the resulted yellow solutions was measured by microplate reader. A series of AFP concentrations (0, 5, 10, 50, 100, and 250 ng/mL) were measured and the results were plotted as optical density (OD) versus AFP concentration (ng/mL).

In the substrate-free study, the biotin-IONPs were incubated with streptavidin-detection antibodies suspended in solution with the weight ratio of IONP:antibody=5:1. The hydrodynamic size of the suspended particles in solution were analyzed by DLS before and after the incubation. Subsequently, the target protein AFP were also added into the mixture for incubation at 36 ℃ for 90 min. The hydrodynamic sizes of the particles were then measured at the end of the incubation, and the biotin-IONP+streptavidin-detection antibody+AFP complexes were imaged by TEM to show the aggregations of biotin-IONPs.

2.4. Investigation of multi-binding of biotin-IONPs with avidin to produce IONP assemblies: In this study, IONP assemblies were produced based on the avidin-induced crosslinking due to the multi-binding of biotin-IONPs to each avidin molecule. In MilliQ water solution, simple biotin-IONP assemblies were produced by incubating the biotin-IONPs with avidin. Three groups of assembles were produced by adding 40, 100, and 200 μg/mL of avidin solution into the same volume of 100 μg IONP/mL biotin-IONP solutions. The control experiments, using BSA to incubate with biotin-IONPs in the same weight ratios were also performed. The extent of the assembly of nanoparticles was determined by DLS. The morphology of the IONP assemblies were also observed under TEM. In addition, a series of biotin-IONP solutions (in MilliQ water) with different concentrations (20, 40, 60, 80, and 100 μg IONP/mL) were also measured by DLS as control samples.

Besides the IONP assemblies produced in simple aqueous solution, it is possible to organize the avidin-induced crosslinking in a water-in-oil microemulsion system. The mixture of chloroform, BSA solution in MilliQ water, and biotin-IONPs was stirred over 18 h to form a water-in-oil microemulsion system. Since that, the biotin-IONPs produced in chloroform solution can be dispersed in both chloroform and water, they can serve as surfactant material in this microemulsion system to encapsulate the micro-droplets of BSA solution. The avidin solution was then dropped into this system slowly to assemble the biotin-IONPs around the micro-droplets. The morphology of the resulted biotin-IONP assemblies was characterized by TEM.

3. Results and discussion: The IONPs synthesized in thermal decomposition were easily dispersed in chloroform to form homogeneous solution. The TEM image in Fig. 1(A) showed that spherical nanoparticles were successfully synthesized. The size distribution histogram (Fig. 1(B)) showed that the IONPs with a diameter of 10.5±0.3 nm had a narrow size distribution. These IONPs were hydrophobic, and after surface modification by biotin, the biotin-

IONPs were hydrophilic. The activity of the biotin content on nanoparticle surfaces were verified by the avidin-HRP induced colorimetrical method. As illustrated by the schematic diagram in Fig. 1 (C), after incubation, the avidin-HRP molecules can specifically tag the biotin-IONPs attracted onto the bottom. Thus, the resulted HRP-induced optical signal (OD) was graphed versus the biotin-IONP concentration (ng/mL). The resulting curve clearly showed that the optical density (OD) increased with the logarithm of biotin-IONP concentration. The control experiment using biotin-HRP did not exhibit any significant optical signal. Consequently, avidin-HRP can bind with biotin-IONPs through the specific avidin-biotin interaction, whereas the biotin-HRP cannot bind with biotin-IONPs through physical absorption. This verified the activity of the biotin content on nanoparticle surfaces, and indicated that such biotin-IONPs are suitable to specifically bind with avidin or streptavidin for the following experiments.

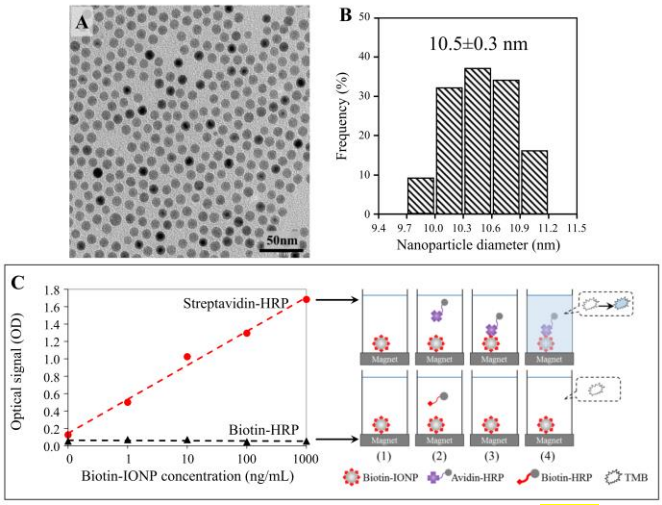

Fig. 1 *(A) TEM image of the synthesized IONPs. (B) The size distribution histogram of IONPs. (C) The result and schematic diagram of the verification experiment of the biotin activity on biotin-IONP surfaces. The result was plotted as optical density (OD) versus biotin-IONP concentration (ng/mL). The schematic diagram showed that only the avidin-HRP could specifically tag the biotin-IONPs and consequently produce gradient OD signal.*

The prepared biotin-IONPs were studied as magnetic labels in the AFP magnetic labeling scheme. The experiments were triplicate and the averaged OD values were plotted into curves versus AFP concentration. In Fig. 2 (A), the results for high (1 μg IONPs/mL), median (0.1 μg IONPs/mL), and low (0.01 μg IONPs/mL) biotin-IONP concentrations were represented by Curve-1, Curve-0.1, and Curve-0.01 respectively. All the three curves exhibited that the OD signal increased with AFP concentration meaning that the sandwich-configured immunoassay of AFP was successfully built. Since that the immunoassay was built before the introduction of biotin-IONP solutions, the quality of the immunoassay for the three experiment groups was not affected by the difference of biotin-IONPs concentrations and were expected to be the same. The differences of the resulting OD signals were caused by the difference of biotin-IONP concentrations. The Curve-1 and Curve-0.1 showed similar increasing tendency. Both these two curves did not show obvious lag phase, the OD signal for 5 ng/mL AFP was significantly different from the background signal obtained from the 0 ng/mL AFP. In addition, they both reached saturation over 100 ng/mL AFP. The only difference is that the data points had lower OD in Curve-0.1 than that in Curve-1. This implies that both the high and median concentrated biotin-IONP solutions can quantitatively label AFP under 100 ng/mL. However, high biotin-IONP concentration can increase the frequency of multi-binding of this original magnetic labels, biotin-IONPs. This resulted in the higher OD signal in Curve-1.

Comparing with Curve-1 and Curve-0.1, the Curve-0.01 exhibited not only much lower OD signal but also different increasing tendency. In Curve-0.01, the 5 ng/mL AFP also showed larger OD signal than that from the 0 ng/mL AFP. However, the OD signal began to reach saturation at only 10 ng/mL of AFP, and reached a complete saturation plateau at 50 ng/mL. This implies that the low biotin-IONP concentration may result in the presence of vacancy on streptavidin-detection antibodies, a part of the streptavidin-detection antibodies were not labeled by biotin-IONPs. By increasing the biotin-IONP concentration up to 0.1 μg IONPs/mL, the vacancy of streptavidin-detection antibodies was avoided. Moreover, by further increasing the biotin-IONP concentration up to 1 μg IONPs/mL, the streptavidin-detection antibodies can be multiple labeled by the biotin-IONPs. Consequently, this biotin-IONP is a promising magnetic label material which can realize the multi-binding of original magnetic labels and quantitatively represent AFP concentration.

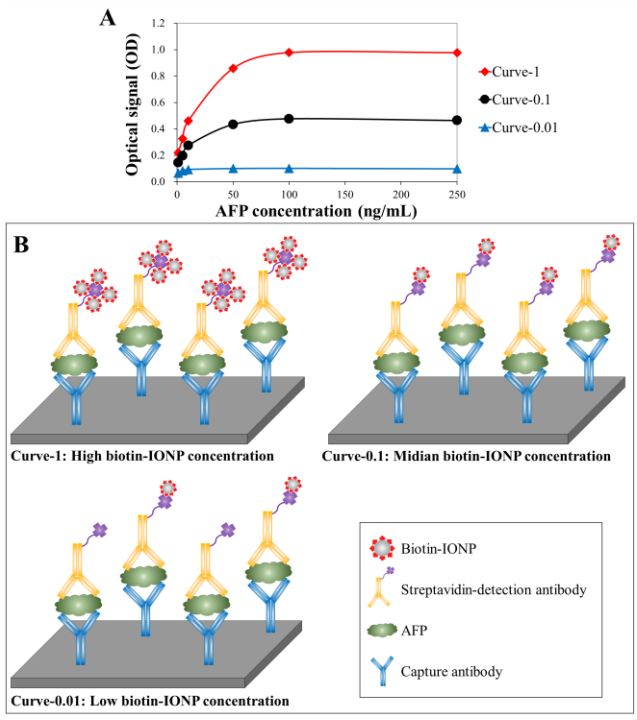

Fig. 2 *(A) The resulting curves of utilizing biotin-IONPs as magnetic labels in AFP magnetic labeling scheme. The Curve-1, Curve-0.1, and Curve-0.01 represent the result from high (1 μg IONPs/mL), median (0.1 μg IONPs/mL), and low (0.01μg IONPs/mL) biotin-IONP concentrations respectively. (B) The schematic diagram illustrates the differences of the three result curves were due to different amount of biotin-IONPs were captured.*

In the substrate-free experiment, the DLS measurement results were shown in Fig. 3 (A) in the form of histogram. The DLS measurement for the dispersed biotin-IONPs in MilliQ water presented a peak of 68 nm. In a previous study, dispersed biotin-IONPs were also produced by the same DSPE-PEG(2000)Biotin addition strategy described in the part 2.2 of this paper [19]. It was reported that the thickness of the organic shell coatings of the biotin-IONPs was around 30 nm. Consequently, in our study the overall diameter of the biotin-IONPs can be estimated as the 30 nm organic shell coatings plus the 10.5 nm

core diameter giving 40.5 nm. The DLS histogram peak of 68 nm is slightly larger than this estimated diameter 41.5 nm because it represented the hydrodynamic size of the dispersed biotin-IONPs. The biotin-IONP dispersion was then deposited onto a copper grid for TEM. Ten locations were randomly selected over the grid for imaging to obtain an overview of the dispersion, and the biotin-IONPs dispersed well over all the observation views. Fig. 3 (B) is one of the representative TEM images showing the dispersed biotin-IONPs. The DLS measurement result agreed well with the TEM observation showing the synthesized biotin-IONPs were well dispersed in MilliQ water as single nanoparticles.

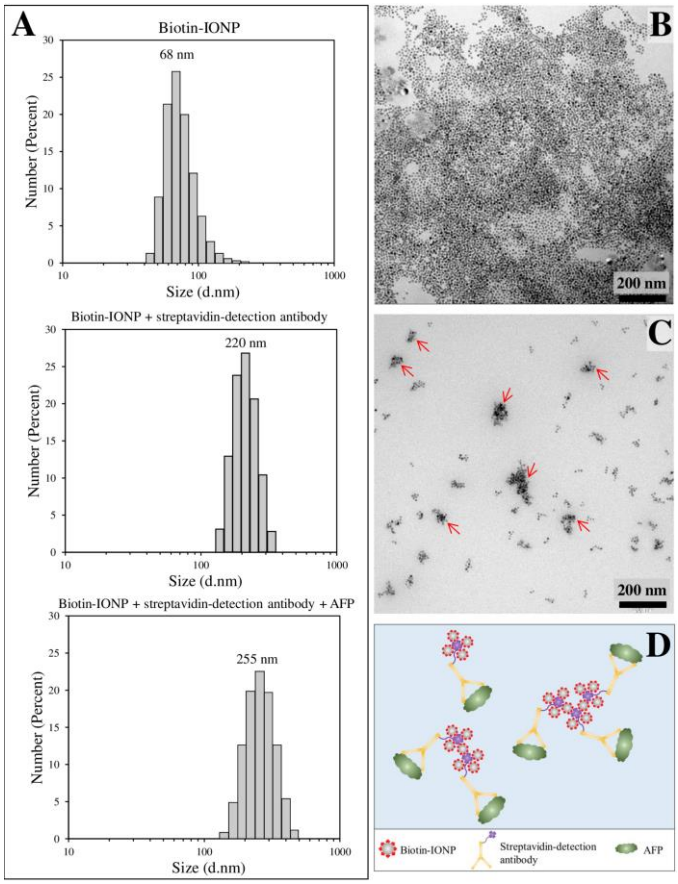

Fig. 3 *(A) DLS measurement results of the single biotin-IONPs, biotin-IONP+streptavidin-detection antibody complex, and biotin-IONP+streptavidin-detection antibody+AFP mixture. (B) TEM image of the dispersed biotin-IONPs. (C) TEM image of the biotin-IONP+streptavidin-detection antibody+AFP mixture. Aggregations of biotin-IONPs were observed (arrows). (D) Schematic diagram of crosslinking of biotin-IONPs caused by streptavidin-detection antibodies in solution. The biotin-IONP aggregations containing one, two, or three streptavidin-detection antibodies are presented as examples.*

After incubation with suspended streptavidin-detection antibodies, the hydrodynamic size was immediately increased. The histogram shows a peak around 220 nm. This is due to the multi-binding of biotin-IONPs onto streptavidin-detection antibodies. Subsequently, AFP was added into this solution, the specific antigen-antibody recognition made detection antibodies bind with AFP. The DLS measurement showed the slightly enlarged hydrodynamic size. The peak of the histogram shifted from 220 nm to 255 nm.

The TEM image in Fig. 3 (C) shows biotin-IONP aggregations due to the multi-binding of biotin-IONP onto each streptavidin-detection antibody. The schematic diagram in Fig. 3 (D) showed the streptavidin-induced crosslinking of biotin-IONPs. Aggregations of biotin-IONPs containing one or multiple streptavidin-detection antibodies can occur. In different situations, the number of streptavidin-detection antibody molecules contained in each biotin-IONP aggregation may be controlled by the concentration of streptavidin-detection antibodies. The real aggregation performance in Fig. 3 (C) seemed to be in different morphologies due to the random arrangement of the streptavidin-detection antibodies and biotin-IONPs. The number of streptavidin-detection antibodies contained into the aggregations was not directly measureable because proteins (streptavidin-detection antibody and AFP) were not visible under TEM; however, the DLS histogram showed a relatively uniform hydrodynamic size distribution of the aggregations suggesting generally the same number of streptavidin-detection antibodies have been involved into each aggregation. By utilizing the multi-binding of biotin-IONPs, it is possible to improve the sensitivity of the substrate-free magnetic biodetection devices. The immune-recognition of the AFP molecules could be sensed by using this biotin-IONP in the substrate-free magnetic biodetection technologies. These biotin-IONPs can also attach to any streptavidin-antibody to produce a specific protein detector.

Table 1: DLS measurement results of the biotin-IONP solutions with different concentrations and biotin-IONP assemblies after addition of different avidin solutions.

Biotin-IONP concentration (μg IONP /mL)	Avidin concentration (μg/mL)	DLS peak (nm)
20	--	68
40	--	68
60	--	68
80	--	68
100	--	68
100	40	255
100	100	342, 1281
100	200	615, 1718

As discussed, the biotin-IONPs suspended well in MilliQ water (Fig. 3 (B)) and the DLS histogram shows a peak of 68 nm representing the hydrodynamic size of dispersed biotin-IONPs. The DLS measurement for a series of biotin-IONP solutions (20, 40, 60, 80, and 100 μg IONP/mL) were then carried out, and generally had the same DLS histogram results with the peak of 68 nm (Table 1). This indicated that the hydrodynamic size measurement was reliable and the biotin-IONPs did not have measurable aggregates in these solutions. Long-term monitoring of biotin-IONPs suspension over one month did not show any obvious change of this hydrodynamic histogram. However, once avidin being added into the biotin-IONP solutions, a rapid increase of the hydrodynamic size happened and the clear solution turned into turbid. Addition of 40 μg/mL avidin solution, the DLS histogram showed the hydrodynamic size increased from 68 nm to around 255 nm. However, when the amount of avidin was increased to 100 μg/mL, two larger hydrodynamic size peaks of 342 nm and 1281 nm appeared. When the added avidin solution was 200 μg/mL, the histogram of the DLS measurement showed two peaks with large size, 615 nm and 1718 nm respectively. The large hydrodynamic sizes were arisen from the avidin induced biotin-IONP assemblies. The TEM images of these three samples were shown in Fig. 4 (B), (C),

and (D) respectively. The biotin-IONP assemblies were all observed in these three samples, and the size increases with the amount of avidin added to the sample. These correlate with the DLS measurement results (Table 1).

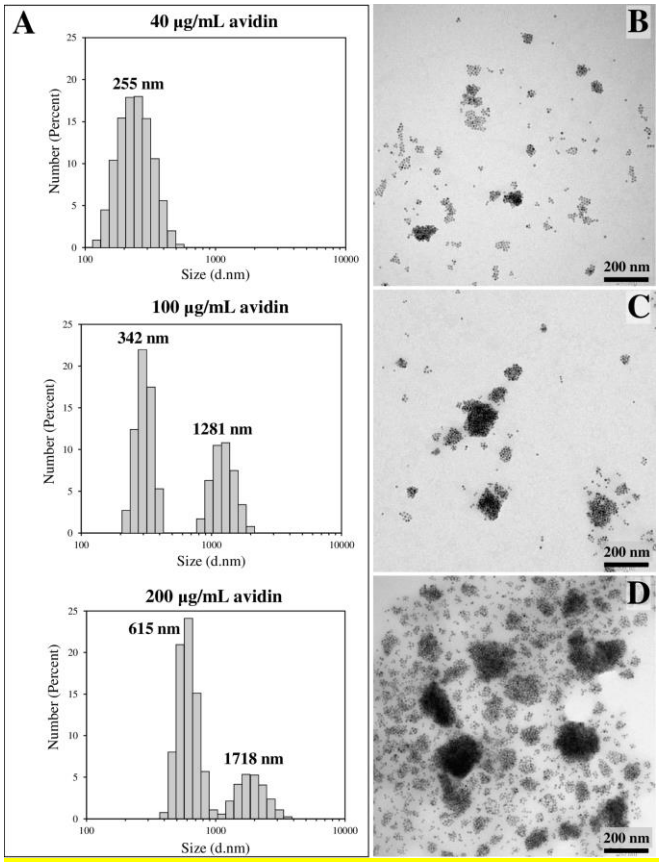

Fig. 4 *(A) DLS measurement results of the biotin-IONP assemblies after addition of avidin. TEM images of the biotin-IONP assemblies formed in the MilliQ water solution after adding (B) 40 µg/mL, (C) 10 µg/mL, and (D) 200 µg/mL of avidin solutions.*

In principle, the tetrameric structure of avidin provides four binding sites for biotin, so more than one biotin-IONPs can bind with each avidin molecule. At the beginning of adding avidin into biotin-IONP solutions, the multi-binding of biotin-IONP with a part of the avidin molecules resulted in small biotin-IONP assemblies. Subsequently, with the help of the remaining available avidin molecules, the small biotin-IONP assemblies can grow by crosslinking with single biotin-IONPs or other biotin-IONP assemblies. Once all the avidin molecules have been used up, the growing process stops. This biotin-IONP crosslinking effect was not observed when biotin-IONPs were incubated with BSA. Biotin-IONPs did not aggregate in the absence of avidin.

The biotin-IONP assemblies produced in the MilliQ water were in the form of condensed nanoparticle aggregations. This should be the result of the random 3D organization of the biotin-IONPs in these assemblies. On the contrary, the biotin-IONP assemblies produced in the water-in-oil microemulsion system show a different morphology in the TEM image (Fig. 5). Generally, the biotin-IONP assemblies were formed in a spherical-like shape. On the edge of the sphere, the biotin-IONPs were relatively densely organized, while the nanoparticle density in the central area was lower than the edge. This suggested there might be a cavity surrounded by the biotin-IONPs in solution, and the biotin-IONP assemblies might be microsphere cages (inset in Fig. 5). Similar vesicle structures assembled from gold nanoparticles have been reported in previous studies [21, 22]. The TEM image of the vesicles also showed spherical ensembles of nanoparticles with a clear contrast between the periphery and the interior, which is characteristic for hollow structures with a large cavity.

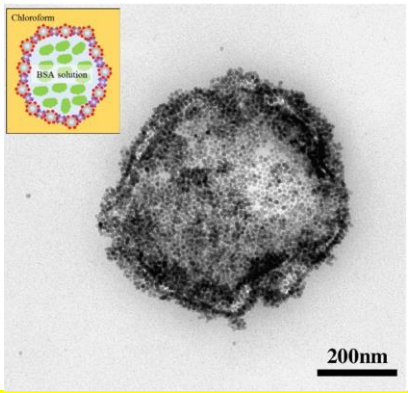

Fig. 5 *TEM image of the biotin-IONP assemblies produced in the microemulsion system. The inset is the schematic cross section of a biotin-IONP microsphere cage formed in the microemulsion system.*

Comparing with the single dispersed magnetic nanoparticles, the magnetic nanoparticle assemblies can cause enhanced T2 relaxation effect in MRI [4], and have a higher response to magnetic field as magnetic drug carrier [5]. Therefore, the condensed biotin-IONPs assemblies produced in MilliQ water have the potential to be developed into MRI contrast agents. The biotin-IONP assemblies produced in the microemulsion system have the potential to encapsulate therapeutic agents inside the assemblies, and thus, can be studied as magnetic drug carriers in the future.

As studied in this paper, the multi-binding of biotin-IONPs with streptavidin-detection antibody and avidin have been investigated. As magnetic labels, the biotin-IONPs can realize the multi-binding in both substrate-based and substrate-free magnetic biolabeling scheme. This makes biotin-IONP a promising magnetic label to improve the sensitivity of magnetic biodetection. In addition, the avidin-induced biotin-IONP assemblies were also produced in MilliQ water and water-in-oil microemulsion system. The magnetic IONP assemblies can produce higher magnetic signal and thus exhibit larger response to applied magnetic field. As a result, these assemblies have the potential to be further studied in biomedical applications such as MRI and magnetic drug delivery. In conclusion, the multi-binding nature of biotin-IONP made it a promising versatile material for magnetic bioapplications.

4. Conclusion: In this study, monodisperse IONPs with 10.5±0.3 nm diameter were successfully synthesized. The surface modification of IONPs with biotin was accomplished by a surfactant addition approach, and biotin-IONPs were prepared. The avidin-HRP can bind with biotin-IONPs through the avidin-biotin reaction, which verified the specific binding activity of the biotin content on biotin-IONP surfaces. These biotin-IONPs were then tested as magnetic labels on a 96-well microplate. The concentration level of the target protein, AFP, was quantitatively represented by the captured biotin-IONPs. By increasing the concentration of applied biotin-IONP solution, the multi-binding of magnetic labels (biotin-IONPs) to streptavidin-detection antibodies took place. The multi-binding of biotin-IONPs with streptavidin-detection antibodies suspended in solution was also observed in TEM. Consequently, by adopting biotin-IONPs as

magnetic labels, the multi-binding of original magnetic labels can be realized in both substrate-based and substrate-free magnetic biodetection.

Taking advantages of the multi-binding nature of biotin-IONPs, the biotin-IONP assemblies were also produced by introducing avidin. The condensed biotin-IONP assemblies were produced in MilliQ water solution. In water-in-oil microemulsion system, the biotin-IONPs were assembled into microsphere cages. By engineering the multi-binding of biotin-IONPs with streptavidin functionalized antibodies or avidin, these biotin-IONPs can be an important versatile material for the future biomedical applications.

5. Acknowledgments: This research is supported by the Seed Funding Program for Basic Research, Seed Funding Program for Applied Research and Small Project Funding Program from the University of Hong Kong, ITF Tier 3 funding (ITS-104/13, ITS-214/14), and University Grants Committee of Hong Kong (AoE/P-04/08).

References:

[1] Wu, W., Wu, Z., Yu, T., et al.: 'Recent progress on magnetic iron oxide nanoparticles: synthesis, surface functional strategies and biomedical applications', Sci. Technol. Adv. Mater., 2015, 16, pp. 023501

[2] Bakshi, M. S.: 'Nanoshape control tendency of phospholipids and proteins: protein–nanoparticle composites, seeding, self-aggregation, and their applications in bionanotechnology and nanotoxicology', J. Phys. Chem. C, 2011, 115, (29), pp. 13947-13960

[3] Bakshi, M. S.: 'Nanotoxicity in Systemic Circulation and Wound Healing', Chem. Res. Toxicol., 2017, 30, (6), pp. 1253–1274

[4] Wu, M., Zhang, D., Zeng, Y., et al.: 'Nanocluster of superparamagnetic iron oxide nanoparticles coated with poly (dopamine) for magnetic field-targeting, highly sensitive MRI and photothermal cancer therapy', Nanotechnology, 2015, 26, pp. 115102

[5] Burnand, D., Monnier, C. A., Redjem, A., et al.: 'Catechol-derivatized poly(vinyl alcohol) as a coating molecule for magnetic nanoclusters', J. Magn. Magn. Mater., 2015, 380, pp. 157–162

[6] Wang, S. X., Li, G.: 'Advances in giant magnetoresistance biosensors with magnetic nanoparticle tags: review and outlook', IEEE Trans. Magn., 2008, 44, (7), pp. 1687-1702

[7] Strömberg, M., Zardán Gómez de la Torre, T., Göransson, J., et al.: 'Multiplex detection of DNA sequences using the volume-amplified magnetic nanobead detection assay', Anal. Chem., 2009, 81, (9), pp. 3398-3406

[8] Choi, J., Gani, A. W., Bechstein, D. J. B., et al.: 'Portable, one-step, and rapid GMR biosensor platform with smartphone interface', Biosensors and Bioelectronics, 2016, 85, pp. 1-7

[9] Østerberg, F. W., Rizzi, G., Torre, T. Z. G., et al.: 'Measurements of Brownian relaxation of magnetic nanobeads using planar Hall effect bridge sensors', Biosensors and Bioelectronics, 40, (1), pp. 147-152

[10] Hao, R., Xing, R., Xu, Z., et al.: 'Synthesis, functionalization, and biomedical applications of multifunctional magnetic nanoparticles', Adv. Mater., 2010, 22, (25), pp. 2729-2742

[11] Gaster, R. S., Hall, D. A., Nielsen, C. H., et al.: 'Matrix-insensitive protein assays push the limits of biosensors in medicine', Nat. Med., 2009, 15, (11), pp. 1327-1332

[12] Wilchek, M., Bayer, E. A.: 'The avidin-biotin complex in bioanalytical applications', Anal. Biochem., 1988, 171, (1), pp. 1-32

[13] Strömberg, M., Torre, T. Z. G., Nilsson, M., et al.: 'A magnetic nanobead-based bioassay provides sensitive detection of single- and biplex bacterial DNA using a portable AC susceptometer', Biotechnol. J., 2014, 9, pp. 137–145

[14] Hassen, W. M., Chaix, C., Abdelghani, A., et al.: 'An impedimetric DNA sensor based on functionalized magnetic nanoparticles for HIV and HBV detection', Sen. Actuators, B, 2008, 134, (2), pp. 755-760

[15] Fu, A., Hu, W., Xu, L., et al.: 'Protein-Functionalized Synthetic Antiferromagnetic Nanoparticles for Biomolecule Detection and Magnetic Manipulation', Angew. Chem. Int. Ed., 2009, 48, (9), pp. 1620-1624

[16] Amstad, E., Textor, M., Reimhult, E.: 'Stabilization and functionalization of iron oxide nanoparticles for biomedical applications', Nanoscale, 2011, 3, (7), pp. 2819-2843

[17] Liljeström, V., Mikkilä, J., Kostiainen, M. A.: 'Self-assembly and modular functionalization of three-dimensional crystals from oppositely charged proteins', Nat. Commun., 2014, 5, pp. 1-9

[18] Li, L., Ruotolo, A., Leung, C. W., et al.: 'Characterization and bio-binding ability study on size-controllable highly monodisperse magnetic nanoparticles', Microelectronic Eng., 2015, 144, pp. 61-67

[19] Xie, J., Peng, S., Browser, N., et al.: 'One-pot synthesis of monodisperse iron oxide nanoparticles for potential biomedical applications', Pure Appl. Chem., 2006, 78, (5), pp. 1003–1014

[20] Uotila, M., Ruoslahti, E., Engvall, E.: 'Two-site sandwich enzyme immunoassay with monoclonal antibodies to human alpha-fetoprotein', J. Immunol. Methods, 1981, 42, (1), pp. 11-15

[21] Bollhorst, T., Rezwan, K., Maas, M. 'Colloidal capsules: nano- and microcapsules with colloidal particle shells', Chem. Soc. Rev., 2017, 46, pp. 2091-2126

[22] Song, J., Fang, Z., Wang, C., et al.: 'Photolabile plasmonic vesicles assembled from amphiphilic gold nanoparticles for remote-controlled traceable drug delivery', Nanoscale, 2013, 5, (13), pp. 5816-5824